The proximity effect in quasars and its applications

Michele Fumagalli - Ay230

December 9, 2008

The proximity effect

The "inverse effect"

Multiple absorption lines are observed blueward of the Lyman-α (Lyα) continuum in quasar (QSO) spectra, caused by several neutral hydrogen rich clouds that lie in the quasar line of sight. According to the observations, the number of clouds per unit redshift can be empirically parametrized with a power law

$$\frac{df}{dz} = A(1+z)^{\gamma} \, . \tag{1}$$

Inspecting individual QSO spectra, Carswell et al. (1982) noticed an "inverse effect" in this distribution: despite for $\gamma > 0$ the number density increases as the redshift increases, as far as one approaches the QSO, the observed cloud density is lower than what expected according to equation (1). A physical explanation for this inverse effect has been firstly proposed by Bajtlik et al. (1988) who argued that bright QSOs may photoionize the nearby clouds, reducing the observed number of absorbers; due to the geometrical nature of this effect, they suggested proximity effect as a more appropriate name. The hypothesis by Bajtlik et al. naturally arises from the fact that QSOs have an abundant UV emission; integrating over their energy distribution, typically described by a power law $f(\nu) \propto \nu^{-1.5}$ at $\lambda < 1216$ Å, it turns out that the total UV emissivity is the dominant contribution to the UV radiation background up to redshift $z = 3.5$ and provides up to an half of the ionizing radiation in the redshift range $4.5 < z < 6$ (Meiksin (2005)).

The photoionization model

In their paper, Bajtlik et al. propose a simple model for the photoionization due the QSO UV photon flux. The neutral gas column density N observed in clouds near a quasar differs from the expected column density N_0 by a factor

$$N = N_0(1+\omega) \, , \tag{2}$$

where

$$\omega = \frac{F_{\nu}^{Q}}{4\pi J_{\nu}} \, . \tag{3}$$

Here J_{ν} is the Lyman-limit background radiation intensity at the redshift z of the absorber, while F_{ν}^{Q} is the local Lyman-limit flux due to the QSO emission. The meaning of equations (2) and (3) is straightforward: the ionization fraction observed in the hydrogen clouds increases when a quasar is close enough so that its flux is at least of the same order of the background field.

Assuming the following distribution of the observed cloud number in the column density space

$$\frac{df}{dN} \propto N^{-\beta} \, , \tag{4}$$

since $\beta > 1$, the number of clouds with a column density greater than a fixed value N_c is $f(N > N_c) \propto N_c^{1-\beta}$; therefore, taking into account the proximity effect, the redshift distribution of the clouds becomes

$$\frac{df}{dz} = A(1+z)^{\gamma}(1+\omega)^{1-\beta}\,, \tag{5}$$

where $\omega = \omega(F_\nu^Q, J_\nu, z, z_Q)$ is a function of the quasar flux, of the UV background flux, of the cloud redshift z and of the quasar redshift z_Q; moreover, ω has a cosmological dependence on Ω, but not on the Hubble constant.

To test the validity of the proximity effect hypothesis, this model can be compared to the observed absorption distribution, after that a few free parameters in the equation (5) are constrained through independent observations; alternatively, it is possible to keep them as free parameters and fit their value to the data. In the original work by Bajtlik et al., it is assumed $\beta = 1.7$, $A = 3.0$ and $\gamma = 2.4$, but the most recent fits to high resolution spectra show that $\beta = 1.5$ for $1.5 < z < 4$ (Kim et al. (2001)), $A = 2.21$ and $\gamma = 2.04$ (Dall'Aglio et al. (2008)). To compute ω, the quasar flux is measured on the spectra and a value for the UV background can be inferred from theoretical models.

Following the argument in the Bajtlik et al. paper, the UV background can be obtained from the UV emission from the QSO, integrated over the quasar luminosity function. Assuming that the quasar luminosity evolves as

$$L(z) = \tilde{L}g(z) \tag{6}$$

with $\tilde{L}$ the present luminosity and $g(z)$ the function which accounts for the cosmological evolution, the QSO luminosity function becomes

$$\rho(z, L) = \frac{\rho_0}{L_*}g(z)^{\alpha-1}\left(\frac{L}{L_*}\right)^{-\alpha} \tag{7}$$

with ρ_0, L_*, and α free parameters; the supply rate of photons of frequency ν from the quasars is therefore

$$S_\nu(z) = \frac{L_*}{h\nu}\left(\frac{\nu}{\nu_r}\right)^{\mu}\int_{Lmin}^{\infty} dL\rho(z, L)\left(\frac{L}{L_*}\right) \tag{8}$$

with μ a known spectral index and ν_r a reference frequency. Assuming that quasars light up at z_{on}, the integrated background radiation becomes (Ikeuchi & Ostriker (1986))

$$J_\nu(z) = \frac{h\nu c}{4\pi}(1+z)^{3-\mu}\int_z^{z_{on}} dz\frac{S_\nu(z)}{H(1+z)^{1-\mu}}\,. \tag{9}$$

Once the ionizing background is fully described, the photoionization model is finally complete and it can be compared with the observations; there are several ways in which this comparison can be done, but the most robust test to prove the validity of the proximity effect hypothesis is through the distribution of the absorbers as a function of ω.

Defining the coevolving redshift integral as

$$X_\gamma = \int (1+z)^{\gamma} dz\,, \tag{10}$$

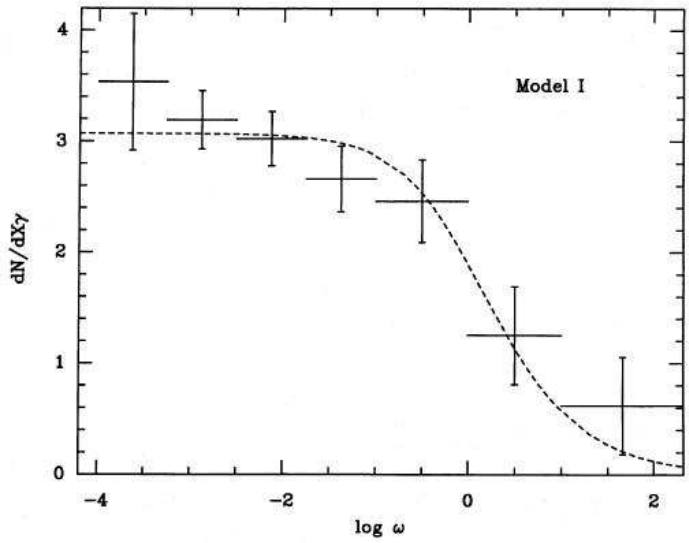

Figure 1: The density of the observed *Lyα* absorbers in coevolving redshift as a function of ω. The dashed line is the prediction of the ionization model. (Bajtlik et al. (1988))

equation (5) becomes

$$\frac{df}{dX_\gamma} = A(1+\omega(z))^{1-\beta}\,; \tag{11}$$

in this way the explicit redshift dependence has been removed, allowing a distance independent way to study the effect due to the ω parameter. In order to compare this parameter with the absorbers distribution, ω is determined assuming the UV background flux as described in the previous section and measuring the QSO flux, while $\frac{df}{dX_\gamma}$ is derived stacking the observed distribution f for individual quasars in each ω bin. Figure 1 shows a comparison between the expected and observed values of $\frac{df}{dX_\gamma}$ as a function of ω. The good agreement ($\chi^2 = 2.99$) between the data and the model clearly proves that the decline of the number of *Lyα* systems seen in the vicinity of the quasars is due to an excess in the ionizing radiation from the QSO which reduces the neutral hydrogen content in nearby clouds.

Probing the high-redshift universe via the proximity effect

Demonstrated the validity of the photoionization hypothesis at the origin of the proximity effect, the analytical model (11) can be used to probe the physics of the high redshift universe, mainly the ionization background, the properties of the QSOs themselves and

of their host galaxies.

The UV background and its evolution

The UV background (UVB) that pervades the IGM is the overall UV emission by different sources. Among the different ways in which the UVB can be predicted or measured[1], the proximity effect offers the most direct approach. The idea is to estimate the UV intensity through a fit of the equation (11) to the observed ω distribution, where J_ν is left as a free parameter; to illustrate with some details this procedure, a review of the recent UVB determination by Dall'Aglio et al. (2008) is presented in this section.

Nowadays, high resolution spectrographs (UVES at VLT or HIRES at Keck) provide large enough sample of QSO spectra to allow a statistical study of the proximity effect. Fitting a power law $f_\nu \propto \nu^\alpha$, the quasar flux at the Lyman limit is measured and the continuum is constrained; the quasar redshift is obtained from the position of metal lines, typically low ionization transitions (SiII+OI) that, being far from the broad line region, avoid a possible redshift uncertainty which rises from the fast relative motion of gas near the AGN. Although high resolution spectra allow high precision line counting in the *Ly*α forest and thus a determination of $\frac{df}{dz}$, the method based on the number density of clouds as used by Bajtlik et al. is replaced by the flux transmission statistic; this avoid the line blending and any bias due to the fitting procedure.

The overall technique is equivalent to the one exposed in the previous sections by replacing the density function f with the effective optical depth τ_{eff}, related to the mean transmission according to

$$\tau_{eff} = -\ln\langle e^{-\tau_{HI}}\rangle \,, \tag{12}$$

where the average $\langle\rangle$ is computed over the redshift intervals. According to this new definition, equation (1) is replaced by

$$\tau_{eff} = \tau_0(1+z)^{\gamma+1} \,; \tag{13}$$

the γ index is measured computing the mean τ_{eff} in the forest of all QSOs in a particular slice of redshift, after the decontamination from damped *Ly*α (DLA) or Lyman limit systems (LLS) and the proximity effect region itself. The proximity effect ξ is then parametrized following the previous derivation, after a redefinition of τ_{eff} to account for the ionising effect due to the quasar:

$$\xi = \frac{\tau_{eff}}{\tau_0(1+z)^{\gamma+1}} = (1+\omega)^{1-\beta} \,. \tag{14}$$

A first determination of the UVB can be done by fitting the observed (ξ,ω) relation for all the QSOs with a model function

$$F(\omega) = \left(1+\frac{\omega}{a}\right)^{1-\beta} \,; \tag{15}$$

[1]For example, similar to what outlined in the previous section, the UVB can be computed numerically given the luminosity function of the UV emitters, their spectral energy distributions and the distribution function of the absorbers in the IGM.

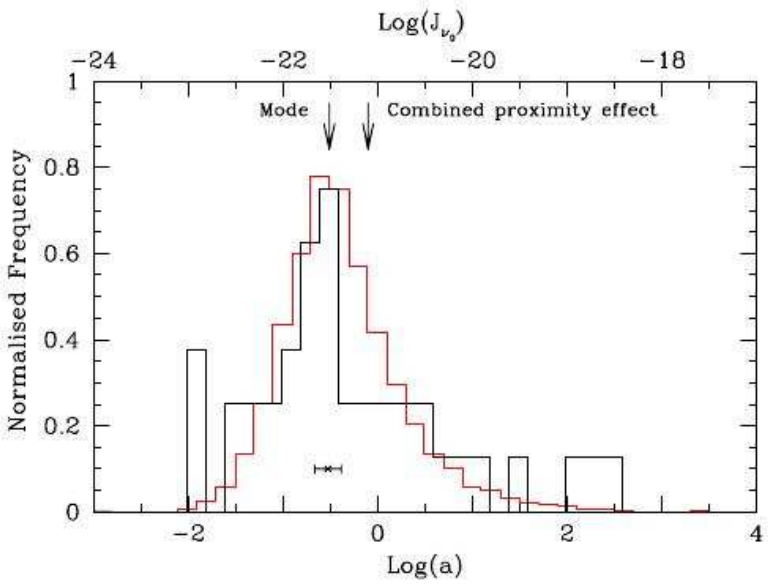

Figure 2: Comparison between the observed (black) and simulated (red) distribution of a from the proximity effect. (Dall'Aglio et al. (2008))

in this equation, a fiducial value $J^* = 10^{-21}$ erg cm^{-2} s^{-1} Hz^{-1} sr^{-1} is assumed so that a is the single free parameter that provides the best fit value for the real background intensity $J_\nu = a \times J^*$, $\log J_\nu = -21.10^{+0.14}_{-0.22}$ (Dall'Aglio et al. (2008)).

Alternatively, instead of stacking ξ in a single plot for all the quasars in the sample, the proximity effect can be detected individually in each line of sight, providing a distribution of a. Figure 2 shows the histogram of these values (thick line) obtained from the sample in Dall'Aglio et al. (2008). Looking at the distribution, it is evident a significant skewness; in addition, these measurements cover a large range of values with a well-defined peak. The observed shape in the distribution poses a serious problem in the determination of the true a while adding all the data together; in particular the tail biases the final UVB towards an higher value, up to a factor of 2.

However, generating simulated spectra with a Monte Carlo simulation, it is possible to quantify and characterise this bias, studying the simulated distribution for a (red line in Fig. 2); in particular, comparing the two sets it turns out that the observed distribution is well describe by a Poisson function that takes into account a pure random variation for different lines of sight. In addition, since it is evident that the modal value for the simulated distribution is the closest number to the expected value, the mode of the observed distribution leads to an unbiased estimation for the UVB: $J_\nu = -21.51 \pm 0.15$.

A possible additional bias may rise when the observed quasar is located in overdensities since in that case the proximity effect will be naturally weakened due to a compensation effect, leading to an overestimate of J_ν. To quantify this bias, an over-

density parameter Ξ can be defined for each line of sight as the ratio between the observed effective optical depth, once correct for the proximity effect, and the expected value, according to equation (13) that does not take into account clustering near the quasar; a global Ξ is computed merging values for individual quasars. Studying this new parameter, Dall'Aglio et al. find that typically quasars reside in denser regions, a result which is confirmed in other works (e.g. Hennawi & Prochaska (2007)); to quantify this effect, they simulated a set of spectra to be compared with observations. Their results show that if all the QSOs observed lied in denser regions, then the observed value for a would be rigidly shifted towards higher values, keeping constant the shape. However, this condition is highly unlikely since it is expected that QSOs reside within environment with different degree of overdensity, a fact that adds a weak broadening in the observed distribution for a.

Due to these biases, the best estimate for the UVB is obtained identifying the outliers in the Ξ distribution, starting from an initial guess on J_ν derived without any correction; after that these QSOs are excluded from the sample, the stacked ξ parameter can be fitted to obtain the best a value. Finally there is the correction for the shift produced by the Poission fluctuation. Following this procedure, the best value for the UVB becomes $\log J_\nu = -21.49^{+0.14}_{-0.21}$ (Dall'Aglio et al. (2008)).

Ideally, by performing this entire analysis in bins of redshift, the dependence of the UVB as a function of z can be described; according to Dall'Aglio et al.:

$$\log J_\nu(z) = (-0.20 \pm 0.14)z + (-21.0 \pm 0.4)\,; \tag{16}$$

however, since the slope is very shallow and the uncertainties in the procedure are large, this law should be considered with some cautions.

Quasar probing quasar

The observed reduction in the absorption features in a QSO spectrum occurs along the line of sight as one approaches the quasar; however, if another QSO lies close to this line of sight, it can locally enhance the photoionization rate above that due to the average cosmic ionizing background, leading to the so-called transverse proximity effect. The study of this effect is worthwhile to understand properties of the quasars themselves and of their host galaxies, as it is described in the following sections.

Quasar environment, variability and anisotropy

From a comparison between the transmitted flux distribution observed in system of quasar pairs and the expected value from artificial absorption spectra generated from cosmological simulation of the *Ly*α forest, information on the clustering, on the variability and on the anisotropy of quasars can be obtained.

One of the first attempt in this direction has been made by Schirber et al. (2004) who studied the transverse proximity effect in three QSO systems, selected to be the closest pairs in the SDSS Early data release with the largest ratio of the ionizing rate from the foreground quasar Γ_f to that of the background ionizing rate Γ_{bkg}. After the continuum emission from the QSO spectra is fitted, the fraction of transmitted flux F

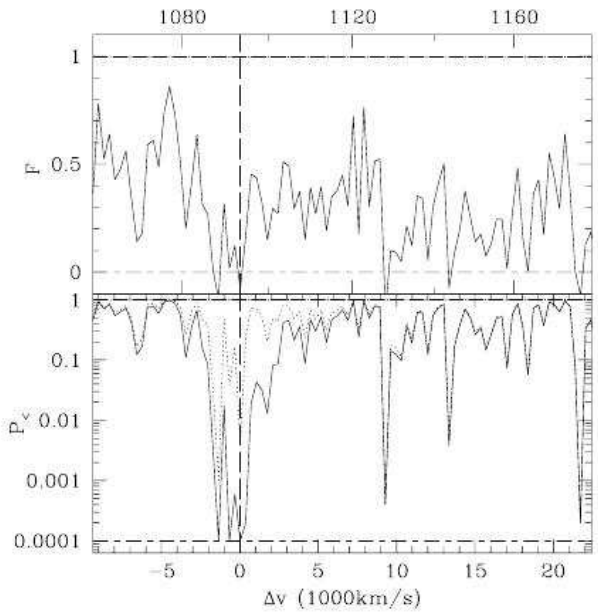

Figure 3: Top: Observed transmitted flux. Bottom: Fraction of simulated spectra with transmitted flux below the measured value with (solid line) or without (dashed line) accounting from the foreground quasar emission. (Schirber et al. (2004))

is measured dividing the observed emission by the continuum flux; this quantity is a direct estimator of the effective opacity due to the absorbers $\tau_{eff} = -\ln(F)$. Similarly to what happens in the proximity effect, along the line of sight the flux emitted by the foreground quasar varies the optical depth by a factor $1+\omega$, where $\omega = \frac{\Gamma_f}{\Gamma_{bkg}}$, with Γ_{bkg} known from independent derivation of the UVB as described in the previous sections; Γ_f is instead directly obtained from the observed flux $F_f(\nu, z)$ according to

$$\Gamma_f = \int_{\nu_0}^{\infty} d\nu \frac{F_f(\nu, z)\sigma_h(\nu)}{h\nu} \tag{17}$$

with σ_h the hydrogen photoionization cross section.

Once ω is known, a synthetic population of absorbers can be simulated within a CDM cosmology for a given bias and primordial spectral index; from this population, a set of simulated spectra with or without the foreground quasar can be generated. Figure 3 shows in the top panel the observed transmitted flux F and in the bottom panel the fraction $P <$ of the simulated spectra in which the transmitted flux is below the measured value in the observed spectrum for the pair J110819-005823 J110813-005944. The solid line includes the emission from the foreground quasar, while the dashed line refers only to the background emission. The fact that at the velocity corresponding with the foreground quasar $P <$ is close to zero proves that the transverse proximity effect is not detected in this case. A similar behaviour is seen in the other two pairs studied

by Schirber et al. (2004), where there is no evidence for an increase in the transmitted flux.

A possible explanation for the absence of the transverse proximity effect is that the adopted cosmological simulation underestimates by a factor of 3-10 the number of absorbers with high column density; in fact, the presence of a significant number of clouds with density $10^{15}(1+\omega)$ cm^{-2} can provide enough source of opacity to compensate for the quasar ionization. However, even correcting for a reasonable number of high column density clouds, the simulated fraction of transmitted flux remains lower than the observed one. Furthermore, inspecting the spectra, there is no evidence of big absorption features along the line of sight. Therefore, the absence of the transverse proximity effect can be attributed to the physical properties of the foreground QSO itself and to its environment.

First of all there are both observations (Ellingson et al. (1991)) and models (Kauffmann & Haehnelt (2002)) according to which clustering can play an important role; in fact, the halo of the QSO has a density enhancement of absorbers that increases the optical depth up to a factor of 2 and therefore it can compensate for the foreground QSO ionization. Nevertheless, this is not enough to account for a reduction of $(1+\omega) \simeq 90$ as observed in the pair J110819-005823 J110813-005944, so other effects should be added to explain the amount of the observed transmitted flux; in other words, it is possible that the reduction in the absorption expected from the transverse proximity effect has been mitigated by the enhance density around the foreground quasar, but clustering itself seems unable to account for the lack of this effect.

Another possible explanation to account for this non detection of the transverse proximity effect is related to the QSO anisotropy; clearly in a flux–limited survey quasars which have very bright emission in the same direction of the line of sight are more likely to be observed, but their flux may be fainter in other directions, i.e. towards the regions probed by the background quasars. Studying the geometry of these systems, the beam size of the collimated foreground QSO emission can be constrained; in particular one can study the angle between the line of sight and the direction connecting the QSO and a point associated with a value Δv in the spectra. It turns out that to justify for the observed low probability $P <$ along a wide range of velocities, very narrow beams are required. Even if these angles are too narrow, it seems a reasonable hypothesis that QSOs do not emit isotropically, a fact that partially contribute to the lack of the transverse proximity effect.

Finally, a further contribution to the observed transmitted flux may come from the QSO variability. Due to relativistic effects, there is a time delay between the QSO emission and the formation of the ionized sphere due by the time required by the light to travel far from the QSO

$$\Delta t = \frac{c^{-1}}{R_f + R_p} \tag{18}$$

where $R_f = \sqrt{R_i^2 + R_p^2}$ is the proper distance from the quasar to the observed region with R_i the impact parameter and $R_p = \Delta v / H(z_{qso})$ the separation along line of sight. Studying the proximity effect, it appears the QSO must sustain its luminosity for at least the photoionization timescale of 3×10^4 yr as set by the ionizing background radiation, but there are evidences that QSOs normally shine for periods at lest of 10^7 years in

order to justify the observed size for the ionized regions. However, QSOs may not maintain their luminosity constant in time as they may undergo short repeated period of high luminosity separated by intervals of lower luminosity, as found for instance by Kirkman & Tytler (2008) who prove QSO episodic lifetimes of $\simeq$ 1 Myr. Once again this is not the only effect that accounts for the undetected transverse proximity effect, but it may add a further contribution.

From what described in this section, it appears clearly that the study of the transverse proximity effect is a powerful tool to characterized the physical properties of the QSOs; even from a non detection of this effect, one can study the clustering, the variability and the anisotropy of quasars.

QSO host galaxies

Searching for QSO pairs is a useful technique that allows the use of the background quasar to study not only the properties of the quasars themselves, but also the physics of the foreground quasar's halo. From this kind of study, a complete description of the QSO host galaxies and their surroundings gives information about quenching, feedback and the evolution of massive galaxies. Few examples are the recent works by Hennawi & Prochaska (2007) who study the anisotropic clustering of optically thick absorbers around quasars or by Kim & Croft (2008) who constrain the quasar host halo masses through observations of QSO pairs. In this section the analysis for the pair SDSSJ1204+0221 by Prochaska & Hennawi (2008) is presented; since this kind of study takes advantage of the proximity effect technique to constrain cosmological models of the halo assembly, the details related with the physics of the medium near the foreground quasar are emphasis, being more relevant to the subject of this review.

Currently, different models of the galaxy assembly and evolution offer an explanation for the observed bimodality in the galaxy population as seen in the color-magnitude diagram. During its life, a super massive black hole ($\simeq 10^9 M_\odot$) liberates an enormous amount of energy which contributes to the UV and X background radiation, causes the proximity effect and originates the observed broad line region; moreover, feedback on even larger scales can explain the observed quenching in the star-formation activity seen in massive galaxies. An alternate scenario implies that gas which accretes in massive halos is shock–heated to the virial temperature, a fact that may suppress the star formation; however, it seems that a cold gas accretion can still feed the halo, but a model in which the gravitational energy released during the cosmological contraction heats the gas may provide a suitable mechanism to halt the star formation. To disentangle between these different models is complex, due to the fact that a detailed knowledge of the local gas physics in the halo is required; therefore, QSO pairs become extremely important cosmological laboratories to test these different models for the galaxy evolution.

The system SDSSJ1204+0221 is composed by a background quasar (BG) and a foreground quasar (FG) at $z_{fg} = 2.4360 \pm 0.0005$, as accurately measured from [OIII] lines. The angular separation is $\theta = 13.3''$, corresponding to an impact parameter $R_p = 108$ kpc at $z = z_{fg}$

Studying the high resolution spectrum of the background quasar, an HI absorber at $z = z_{fg}$ can be identify from both $Ly\alpha$ and $Ly\beta$ features. The best fit to the ab-

sorption profiles establishes that this system is composed by three clouds; clouds A and C have a column density $N_{HI} < 10^{19}$ cm^{-2} ($N_{HI} = 10^{18.6}$ cm^{-2} from the best fit) and a Doppler parameter $b < 25$ km s^{-1}, while the cloud B has an higher HI column density $N_{HI} < 10^{19.60}$ cm^{-2} which does not allow a determination for b. Studying the metal-line transitions by fitting Voigt-profiles, further constrains can be added to the kinematic of the system; the three clouds span a velocity interval $\Delta v = 650$ km s^{-1} and all of them have positive values with respect to z_{fg}. This high velocity, unusually large if compared with what observed in the DLA or LLS, probes that the observed gas is subject to extreme kinematic conditions and perhaps to coherent motion.

Additional physical parameters may be derived by studying the ratio of the different ionization states of a same element. The high ratio of the low-ions like N^+/N^0 together with the absence of highly ionized states (SiIV,CIV) reveals that the gas is only partially ionized; this poses a constrain on the gas temperature $10^4 < T < 10^5$ K. By interpreting the observed b-values in N^0 or O^0 as pure thermal motion, it is reasonable to assume $T_e = 20000$ K; in addition, it seems unlikely that a source of energy can keep the gas hot to justify a pure collisional excitation, suggesting that the photoionization is the dominant process. By assuming a photoionization model, in order to reproduce the observed ratio in the low-ions, upper and lower limit can be imposed on the ionization parameter $U = \phi/(n_H c)$, with ϕ the photon flux. Using the most likely value $\log U = -3.0$ dex, the ionization fraction $x = H^+/H$ and the total hydrogen column density $N_H \simeq 10^{20.6}$ cm^2 can be computed. Due to the fact that at $\log U < -2.5$ dex the measured ratio O^0/H^0 is a good estimator for the metallicity, it appears that the observed gas is metal rich (at least 1/10 solar abundance); in addition, after the ionization correction for O/Fe and N/O, the observed ratio suggests that the gas is metal enriched. Oxygen is synthesized in massive stars in a very short timescale, while nitrogen and iron are associated with Type Ia SN, a fact that causes a delay in the emission of these elements up to 1 Gyr. Therefore, the relative distribution of these elements constrains the star formation history, once differential depletion has been taken into account: the observed metal distribution suggests a star formation history typical of bright spheroidal, compatible with a short period of intense star formation within 100 Myr and 1 Gyr.

All together, the observed extreme kinematic, the high metallicity and a solar N/O ratio suggest that this system is connected with the foreground quasar within the impact parameter, as confirmed also by the probability distribution function from the observed strong clustering of optically thick absorbers around $z \simeq 2$ quasars (Hennawi & Prochaska (2007)).

Additional information of the physics near the foreground quasar comes from the absence of high ions transitions, a fact that constrains the nature of the diffuse hot gas in the halo. In fact, from the low column density of C^+, N^{+4} or O^{+5} it's clear that the line of sight does not intersect a large column density of warm $T \simeq 10^5 - 10^6$ material; moreover, the temperature dependence of O^{+5} for the collisional excitation equilibrium establishes that a diffuse shock heated medium in the halo must have $T > 10^6$ K, consistent with the virial temperature in the gas of a massive halo ($M > 10^{13} M_\odot$).

The absence of high-ion transitions is also a first hint that the foreground QSO emits anisotropically as typically observed in quasars (Schirber et al. (2004)) and there are other evidences that the foreground QSO is not shining towards the observed gas

region. Assuming $T_e = 20000$ K, the observed population of the fine-structure levels of Si^+ and C^+ gives an estimation for the electron density n_e which, combined with the ionization fraction x, allows a determination of the hydrogen volume density $n_H = n_e/x$. Assuming $n_H < 1$ cm^{-3} and $\log U < -4$ dex, an upper limit on the ionizing photon flux is set to $\phi_{obs} = 3 \times 10^6$ photons s^{-1} cm^{-2}; since the foreground quasar photon flux is $\phi_{fg} = 9 \times 10^7$ photons s^{-1} cm^{-2} as computed from the observed luminosity assuming isotropic emission, one should require that the gas is located at a distance $r > 500$ kpc in order to maintain the isotropic emission hypothesis; however, the clustering of absorbers around quasars implies a distance $r \simeq 100$ kpc, close to the impact parameter. In addition, if the gas was illuminated by the quasar, one would expect $Ly\alpha$ emission which is not observed with a sensitivity greater than a factor of ten than the expected $Ly\alpha$ flux.

Once the properties of the gas have been determined, possible models that describe the physics of the halos can be compared with the observations. Clearly information from one line of sight is not enough to generalize the problem, but some hypothesis on the nature of the observed gas can be done. The main question to be answer is why a cold cloud ($T_e < 20000$ K), highly metal enriched and with extreme kinematic conditions is observed at a distance of 100 kpc away from the quasar. A possible explanation is to associate the observed gas with a large scale outflow or a galaxy wind; however, the energy rate required to transfer material at the distance of the impact parameter is $E_w \simeq 10^{45}$ erg s^{-1}, too high to be attributed to wind originated by the star formation or to the radiation pressure feedback from the quasar. Nevertheless, the ratio between the power of the outflow and the energy provided by the accretion is a few percents; this value is close enough to the value used to reproduce the $M - \sigma$ correlation to corroborate the feedback hypothesis, even if the lack of a warm medium at $T \simeq 10^5 - 10^6$ K remains unexplained. An alternate hypothesis is to relate this gas with material which is either infalling or virialized within the potential well of the massive dark matter halo. In fact, the predicted value of pressure for these clouds matches the expected value for the pressure equilibrium condition in the shock-heated gas in the halo; moreover the observed kinematic reasonably matches the expected one. This hypothesis, even if is able to justify the lack of a warm medium, seems not to be able to predict the observed high value of metallicity. Even if a larger sample is required, it appears that this technique is promising to constrain the physics of the halo assembling and evolution.

Bibliography

Carswell, R. F., Whelan, J. A. J., Smith, M. G., Boksenberg, A., & Tytler, D. 1982, MNRAS, 198, 91

Bajtlik, S., Duncan, R. C., & Ostriker, J. P. 1988, ApJ, 327, 570

Meiksin, A. 2005, MNRAS, 356, 596

Kim, T.-S., Cristiani, S., & D'Odorico, S. 2001, AAP, 373, 757

Dall'Aglio, A., Wisotzki, L., & Worseck, G. 2008, arXiv:0807.5089

Ikeuchi, S., & Ostriker, J. P. 1986, ApJ, 301, 522

Kirkman, D., & Tytler, D. 2008, arXiv:0809.2277

Hennawi, J. F., & Prochaska, J. X. 2007, ApJ, 655, 735

Kim, Y.-R., & Croft, R. A. C. 2008, MNRAS, 387, 377

Schirber, M., Miralda-Escudé, J., & McDonald, P. 2004, ApJ, 610, 105

Kauffmann, G., & Haehnelt, M. G. 2002, MNRAS, 332, 529

Ellingson, E., Yee, H. K. C., & Green, R. F. 1991, ApJS, 76, 455

Merritt, D., & Ferrarese, L. 2001, ApJ, 547, 140

Prochaska, J. X., & Hennawi, J. F. 2008, arXiv:0806.0862